Excellent energy storage properties and stability of $NaNbO_3$-$Bi(Mg_{0.5}Ta_{0.5})O_3$ ceramic by introducing $(Bi_{0.5}Na_{0.5})_{0.7}Sr_{0.3}TiO_3$

Hongyun Chen[a], Junpeng Shi[a], Xiuli Chen*, Congcong Sun, Feihong Pang, Xiaoyan Dong, Hailin Zhang, Huanfu Zhou*

Collaborative Innovation Center for Exploration of Hidden Nonferrous Metal Deposits and Development of New Materials in Guangxi, Key Laboratory of Nonferrous Materials and New Processing Technology, Ministry of Education, School of Materials Science and Engineering, Guilin University of Technology, Guilin 541004, China.

[*] **Corresponding authors:**

E-mail addresses: cxlnwpu@163.com (X. Chen), zhouhuanfu@163.com.

[a] These authors contributed equally.

1. Experimental procedures

1.1 Formula.

Generally, the dielectric properties of energy storage ceramic are largely reflected in its W_{rec} and η, which can be given as follows:

$$W = \int_0^{P_{max}} EdP \quad , \tag{1}$$

$$W_{rec} = \int_{P_r}^{P_{max}} EdP \quad , \tag{2}$$

$$\eta = \frac{W_{rec}}{W} \times 100\% \quad , \tag{3}$$

where W is total storage density, P_{max} and P_r are maximum polarization and residual polarization, E is applied electric field. Obviously, the high breakdown field strength (E_b) and P_{max} will be advantageous for the improvement of energy storage performance.

The E_g values can be estimated using Tauc equation:

$$(\alpha h\upsilon)^2 = A(h\upsilon - E_g) \quad , \tag{4}$$

where h, υ and α are the Planck constant, the frequency, and the absorption coefficient, respectively.

1.2 Fabrication of (1-*x*)(0.9NaNbO$_3$-0.1Bi(Mg$_{2/3}$Ta$_{1/3}$)O$_3$)-*x*(Bi$_{0.5}$Na$_{0.5}$)$_{0.7}$Sr$_{0.3}$TiO$_3$ ceramics.

(1-*x*)(0.9NaNbO$_3$-0.1Bi(Mg$_{2/3}$Ta$_{1/3}$)O$_3$)-*x*(Bi$_{0.5}$Na$_{0.5}$)$_{0.7}$Sr$_{0.3}$TiO$_3$ (*x*BNST) ceramics were fabricated via the conventional solid-state reaction method. Na_2CO_3, Nb_2O_5 were weighed as first group, Bi_2O_3, MgO, Ta_2O_5 were weighed as second group, Na_2CO_3, Bi_2O_3, TiO_2, $SrCO_3$ were weighed as third group. Three groups of raw materials were mixed in ethanol with zirconia balls for 4h. After drying, well-mixed powders of first group were calcined at 850 ℃ for 3h in air, powders of the second

group were calcined at 850 ℃ for 2.5h in air. The calcined powders were milled for 4h in the same way as the original powders. The resultant powders were mixed with 6wt% of polyvinyl alcohol (PVA) and pressed into pellets with 8mm in diameter and 1mm in thickness by uniaxial pressing at 10 MPa. The samples were coated with calcined powders of the same composition in order to minimize volatilization of alkaline elements and sintered at different temperatures, depending on the doping content, ranging from 1180 °C to 1280 °C for 2h in the air.

1.3 Characterization

The phase structures of the samples were analyzed using an X-ray powder diffraction (XRD, Model X'Pert PRO; PA Nalytical, Almelo, Netherlands) with Cu K_{α} radiation (λ = 0.15406 nm). The microstructures of the samples were observed via a scanning electron microscopy (Model JSM6380-LV SEM, JEOL, Tokyo, Japan). The relative permittivity and loss tangent of the ceramics were measured using a precision impedance analyser (Model 4294A, Hewlett-Packard Co, Palo Alto, CA) in the temperature range of -200°C to 300°C with the heating rate of 2°C/min. Polarization hysteresis loops were measured via a ferroelectric material parameters tester (RT66, Radiant Technologies, NM, USA). To better characterize the energy storage properties, the sintered samples were polished down to a thickness of 0.15 ± 0.01. Screen printing method was adopted to coated sample via Ag electrode with a diameter of 2 mm. The Raman shifts was measured at room temperature by using Raman tester (XDR, Thermo Fisher Scientific, USA). The dielectric breakdown strength (*BDS*) was measured at room temperature by using a voltage-withstand test device (RK2671AM). Charging

and discharging performances were tested by a dielectric charge test system (CFD-003, TG Technology, Shanghai, China).

1.4 Results and discussion

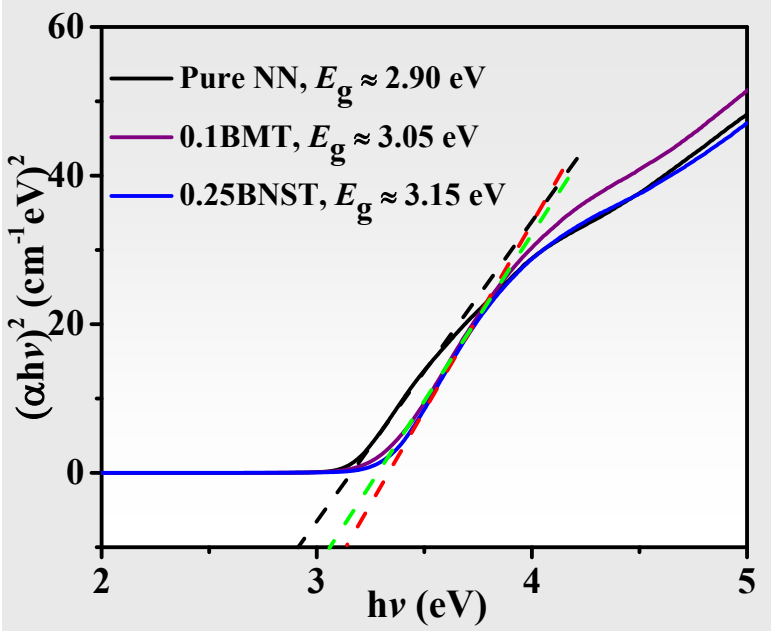

Fig. S1 Energy dependence of $(\alpha h\nu)^2$ for NN, 0.10BMT, 0.25BNST sample.

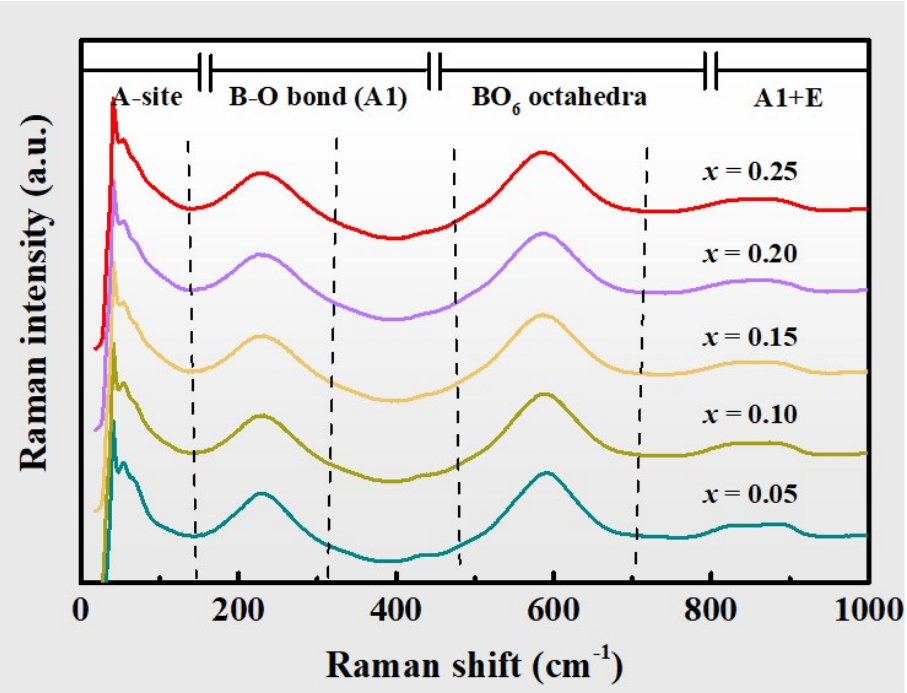

Fig. S2 Raman spectrum of *x*BNST ceramic

Table S1 Comparison of the charge-discharge performance between the 0.25BNST ceramic and several other ceramics.

Composition	C_D (A/cm^2)	P_D (WM/cm^3)	W_D (J/cm^3)	$t_{0.9}$ (ns)	E (kV/mm)	Ref.
$0.85BaTiO_3$-$0.15Bi(Zn_{0.5}Sn_{0.5})O_3$	551	30.3	0.47	160	11	1
$0.85K_{0.5}Na_{0.5}NbO_3$-$0.15(K_{0.7}Bi_{0.3})NbO_3$	794.91	47.69	—	—	12	2
$0.91NaNbO_3$-$0.09Bi(Zn_{0.5}Ti_{0.5})O_3$	356	20	0.48	250	11	3
$0.93Na_{0.5}Bi_{0.5}TiO_3$-$0.07LiTaO_3$	440	22	0.52	100	10	4
$0.9(0.94Na_{0.5}Bi_{0.5}TiO_3$-$0.06BaTiO_3)$ -$0.1NaNbO_3$/ZnO	277.1	—	1.17	256	10	5
$0.92NaNbO_3$-$0.08Bi(Mg_{0.5}Ti_{0.9})O_3/MnO_2$	363.7	63.7	1.17	83	20	6
$0.55Bi_{0.5}Na_{0.5}TiO_3$-$0.45Sr_{0.7}La_{0.2}TiO_3$	1815	182	2.31	123	20	7
$0.72NaNbO_3$-$0.08Bi(Ni_{0.5}Zr_{0.5})O_3$	588.9	41.2	0.68	60	14	8
$0.88BaTiO_3$-$0.12Bi(Ni_{2/3}Nb_{1/3})O_3$	738	39.6	0.54	90	10	9
$0.675NaNbO_3$-$0.075Bi(Mg_{0.5}Ta_{0.5})O_3$ -$0.25(Bi_{0.5}Na_{0.5})_{0.7}Sr_{0.3}TiO_3$	**614.5**	**49**	**0.73**	**32**	**16**	**This work**

References

[1] M.X. Zhou, R.H. Liang, Z.Y. Zhou, X.L. Dong, Novel $BaTiO_3$-based lead-free ceramic capacitors featuring high energy storage density, high power density, and excellent stability, J. Mater. Chem. C. 6 (2018) 8528-8537.

[2] A. Tian, R.Z. Zuo, H. Qi , M. Shi, Large energy-storage density in transition-metal oxide modified $NaNbO_3$–$Bi(Mg_{0.5}Ti_{0.5})O_3$ lead-free ceramics through regulating the antiferroelectric phase structure, J. Mater. Chem. A. 8 (2020) 8352-8359.

[3] Y. Fan, Z.Y. Zhou, R.H. Liang, X.L. Dong, Designing novel lead-free $NaNbO_3$-based ceramic with superior comprehensive energy storage and discharge properties for dielectric capacitor applications via relaxor strategy, J. Eur. Ceram. Soc. 15 (2019) 4770-4777.

[4] L. Zhang, Y.P. Pu, M. Chen, T.C. Wei, X. Peng, Novel $Na_{0.5}Bi_{0.5}TiO_3$based, lead-free energy storage ceramics with high power and energy density and excellent high-temperature stability, Chem. Eng. 383 (2020) 123154.

[5] Y. Yao, Y. Li, N.N. Sun, J.H. Du, X.W. Li, L.W. Zhang, Q.W. Zhang, X.H. Hao, Enhanced dielectric and energy-storage properties in ZnO-doped $0.9(0.94Na_{0.5}B_{i0.5}TiO_3$-$0.06BaTiO_3)$-$0.1NaNbO_3$ ceramics, Ceram. Int. 44 (2018) 5961–5966.

[6] M. Zhang, H.B. Yang, D. Li, Y. Lin, Excellent energy density and power density achieved in $K_{0.5}Na_{0.5}NbO_3$-based ceramics with high optical transparency, J. Alloys Compd. 829 (2020) 154565.

[7] X.S. Qiao, F.D. Zhang, D. Wu, B. Chen, X.M. Zhao, Z.H. Peng, X.D. Rena, P.F. Liang, X.L. Chao, Z.P. Yang, Superior comprehensive energy storage properties in $Bi_{0.5}Na_{0.5}TiO_3$-based relaxor ferroelectric ceramics, J. Chem. Eng. 388 (2020) 12458.

[8] H.Y Chen, X.L. Chen, J.P. Shi, C.C. Sun, X.Y. Dong, F.H. Pang, H.F. Zhou, Achieving ultrahigh energy storage density in $NaNbO_3$–$Bi(Ni_{0.5}Zr_{0.5})O_3$ solid solution by enhancing the breakdown electric field, 10.1016/j.ceramint.2020.07.345.

[9] M.X. Zhou, R.H. Liang, Z.Y. Zhou, X.L. Dong, Combining high energy e□ciency and fast charge-discharge capability in novel BaTiO3-based relaxor ferroelectric ceramic for energy-storage, Ceram. Int. 45 (2019) 3582–3590.